Crystallographic Study of the Binding of Dipeptide Inhibitors to Thermolysin: Implications for the Mechanism of Catalysis†

W. R. Kester and B. W. Matthews*

ABSTRACT: The mode of binding to thermolysin of a number of dipeptide inhibitors including β-phenylpropionyl-L-phenylalanine and carbobenzoxy-L-phenylalanine has been determined by x-ray crystallography to a nominal resolution of 2.3 Å. These results indicate the probable mode of binding of extended substrates to thermolysin and also suggest a mechanism of action for this neutral metalloendopeptidase which is similar in a number of respects to one of the two alternate mechanisms for peptide hydrolysis by carboxypeptidase A proposed by Lipscomb and co-workers (Lipscomb, W. N., et al. (1968), *Brookhaven Symp. Biol. 21*, 24). The crystallographic results suggest that substrates bind to thermolysin with the carbonyl oxygen of the scissile peptide bond displacing a water molecule and becoming the fourth zinc ligand. Also, in the case of β-phenylpropionyl-L-phenylalanine, the side chain of Glu-143 and a neighboring water molecule are seen to be close to the carbonyl carbon of the scissile peptide, as is the imidazole of His-231 to the peptide nitrogen, suggesting that these groups may participate in catalysis. It is proposed that following substrate binding, Glu-143, acting as a general base, promotes the attack of a water molecule on the carbonyl carbon of the scissile peptide bond. Concurrent with, or following this step, His-231 donates a proton to the peptide nitrogen, forming a tetrahedral intermediate which is stabilized by both hydrogen bonds and hydrophobic interactions. Finally, the carbon–nitrogen bond of the intermediate breaks to yield the products. Thus, Glu-143 in thermolysin appears to be a counterpart of Glu-270 in carboxypeptidase A, while the role of His-231 as a proton donor is analogous to that of Tyr-248. The proposed mechanism for thermolysin is similar to that suggested by Lipscomb for carboxypeptidase A in which Glu-270 acts as a general base. In contrast, however, in the case of thermolysin, stereochemical restrictions appear to exclude the possibility of direct nucleophilic attack of the carbonyl carbon by the acid, as occurs in the alternative mechanism of action for carboxypeptidase A proposed by Lipscomb and co-workers.

Thermolysin (TLN)[1] is a heat-stable extracellular endopeptidase of molecular weight 34 600 isolated from *Bacillus thermoproteolyticus* (Endo, 1962). The enzyme binds one zinc ion, required for activity (Latt et al., 1969), and four calcium ions which are necessary for optimal thermostability (Feder et al., 1971). Kinetic studies have shown that TLN specifically hydrolyzes peptide bonds on the imino side of large hydrophobic residues such as leucine, isoleucine, and phenylalanine and that hydrolysis of peptide bonds between two successive hydrophobic residues is most efficient.

The amino acid sequence (Titani et al., 1972) and the x-ray structure to a nominal resolution of 2.3 Å have been determined (Matthews et al., 1972a,b; Colman et al., 1972). Preliminary atomic coordinates are available and are currently being refined (Matthews et al., 1974). In this communication, we describe the mode of binding of several dipeptide inhibitors to the crystalline enzyme and present a mechanism of action which is suggested by these results.

Experimental Section

Materials. Thermolysin, three times recrystallized, was obtained from Calbiochem. Inhibitors, the companies from which they were purchased, and the abbreviations used in this paper follow: L-alanyl-L-phenylalanine (Ala-Phe), Cyclo Chemical; *N*-carbobenzoxy-L-phenylalanine (Cbz-Phe), Cyclo Chemical; L-phenylalanyl-L-phenylalanylamide (PPN), Fox Chemical Co.; L-phenylalanine (L-Phe), Cyclo Chemical. β-Phenylpropionyl-L-phenylalanine (β-PPP) was a generous gift of Dr. B. L. Vallee.

Methods. Native crystals suitable for x-ray diffraction were prepared as described previously (Colman et al., 1972), and kept in a solution of 0.01 M calcium acetate, 0.01 M Tris–acetate, and 5% by volume dimethyl sulfoxide, pH 7.3, used as standard mother liquor in the determination of the native structure. To prepare enzyme–inhibitor derivatives, native crystals were soaked at room temperature in standard mother liquor to which saturating, or nearly saturating, concentrations of the various inhibitors were added and adjusted to pH 7.0. Since binding appeared to be complete after soaking overnight, soaking times were from 2 to 8 days, with the solutions refreshed every 2 days. The concentration used for x-ray analysis and approximate K_I of each inhibitor are given in Table I.

Thermolysin crystallizes in space group $P6_122$, with cell axes $a = b = 94.2$ Å, $c = 131.4$ Å. Data were collected by the photographic method using Enraf-Nonius precession cameras in the same manner as isomorphous derivatives for phase determination. The x-ray source was an Elliot GX-6 rotating anode generator run at 40 kV, 40 mA, and crystals were exposed for 40 h. A summary of the data collection statistics and changes in unit cell parameters is given in Table II.

It was found that the different inhibitors could not be reliably screened using *h0l* projection data alone, because of the small differences observed when inhibitors were bound. Therefore 2.3 Å resolution "subsets" were collected, consisting of 6 planes: *h0l*, *h*1*l*, *hhl*, *h*,*h* − 1,*l*, *hk*0, and *hk*1. Compared with a "full" data set, such a subset contains about a third of

† From the Institute of Molecular Biology and the Departments of Chemistry and Physics, University of Oregon, Eugene, Oregon 97403. *Received December 22, 1976.* This work was supported in part by the National Institutes of Health (GM 20066; GM 15423), by the National Science Foundation (PCM 74-18407), and by a Career Development Award (GM 70585) from the National Institute of General Medical Science to B.W.M.

[1] Abbreviations used: TLN, thermolysin; Ala-Phe, L-alanyl-L-phenylalanine; Cbz-Phe, *N*-carbobenzoxy-L-phenylalanine; PPN, L-phenylalanyl-L-phenylalanylamide L-Phe, L-phenylalanine; β-PPP, β-phenylpropionyl-L-phenylalanine; Tris, tris(hydroxymethyl)aminomethane; rms, root mean square; NMR, nuclear magnetic resonance; DMA, dimercury acetic acid.

TABLE I: Binding Constants for Thermolysin Inhibitors.

Inhibitor	Concn used (mM)	K_I (mM)	Reference
β-PPP	~20[a]	1.6	Holmquist and Vallee (1974)
Cbz-Phe	~20[a]	0.51	Feder et al. (1976)
Ala-Phe	100	~100	Feder et al. (1976); Morihara and Tsuzuki (1970)
PPN	30	~2	Feder et al. (1976)
L-Phe	100	15.6	Feder et al. (1976)

[a] Saturated solution.

the total reflections, including all of the centrosymmetric data, and in space group $P6_122$ provides a reasonably good sampling of reciprocal space. Maps calculated using the subset would be expected to have peaks which are distorted in shape and weaker than those obtained using the full data set, yet still contain many of the features of the full data set map which would not be apparent if a complete set of low resolution data was used. After subset difference maps of all five inhibitors were compared, complete data sets for two of them, β-PPP and Cbz-Phe, were collected. The difference maps using the full data set were found to be in very good agreement with the subset maps.

Due to the fact that the native thermolysin map contains strong density in the active site, attributed to ordered solvent (probably including a Tris molecule), "normal" difference Fourier maps with coefficients of the form $(F_{Deriv} - F_{Nat})$ could not be used reliably for model building. Instead, coefficients of the form $(2F_{Deriv} - F_{Nat})$ were used, and Kendrew–Watson models were built into the electron density maps by use of an optical comparator (Richards, 1968; Colman et al., 1972). Coordinates were determined by placing markers within the appropriate density on the map sections, using the model as a guide. Values of x and y were then measured directly from the map sections and z values estimated to a fourth of a section (0.18 Å).

Final coordinates were obtained by fitting a stereochemically acceptable model to the guide coordinates using the procedure described by Ten Eyck et al. (1976). In this procedure the function

$$\phi = W_1 \sum_i w_i(x_i)^2 + W_2 \sum_{(ij)} w_{ij}(d_{ij})^2$$

is minimized, where x_i is the displacement of atom i from its experimental position and d_{ij} is the deviation of the interatomic distance between atoms i and j from its ideal value. The weights for all atomic displacements, w_i, were given unit value while the weights for bond distances and angles, w_{ij}, were assigned by the following formula: for bonds and angles of planar groups including peptides, carboxyls, and phenyl rings, w_{ij} = 10; for bonds between tetrahedral carbons, w_{ij} = 3; for angles at tetrahedral carbons, w_{ij} = 1. The "global" weights W_1 and W_2 were such that constraints were weighted 100:1 over atomic displacements. Ideal values of bond lengths and angles were taken from the Handbook of Biochemistry (Sober, 1970). The calculation was repeated until the rms deviation from constraints was 0.01 Å. For each inhibitor, the rms atomic movement was about 0.12 Å.

It is difficult to obtain a reliable value for the probable error in the inhibitor coordinates, but we estimate that the maximum error is unlikely to exceed about 0.5 Å and that the average error is probably about 0.2 Å.

TABLE II: Intensity Statistics for Thermolysin Inhibitors.

Derivative	Native	β-PPP	Cbz-Phe	Ala-Phe	PPN	L-Phe
Intensity statistics[a]						
Films	24	22	22	6	6	6
Av R_{sym}	0.054	0.067	0.063	0.069	0.071	0.078
Av R_{sca}	0.053	0.046	0.043	0.042	0.045	0.051
R_{merge}	0.020	0.025	0.022	0.018	0.022	0.038
Av isom diff (%)		7.3	11.9	7.5	6.7	9.2
Reflections	14210	13741	13948	5048	4891	4819
Cell dimensions						
a, b (Å)	94.2	94.2	94.1	94.3	94.3	94.2
c (Å)	131.4	131.5	131.5	131.5	131.5	131.3

[a] The respective R values are as defined previously (Colman et al., 1972; Matthews et al., 1972c).

Results

Binding of β-PPP. β-PPP was found to bind only at the active site of thermolysin. Examination of the $F_{\beta\text{-PPP}} - F_{Nat}$ difference Fourier map revealed strong positive and negative features in the active site region (Figure 1) extending up to three times the height of any feature throughout the remainder of the asymmetric unit. The two strongest positive features, labeled "phe" and "β-phe" in Figure 1, can be attributed to the respective phenyl rings of the inhibitor, but the density between these two positive features is negative, which we interpret as being due to the displacement of ordered solvent, probably including a Tris molecule, from the "native" enzyme. In contrast, the map with coefficients $(2F_{\beta\text{-PPP}} - F_{Nat})$ has continuous positive density for the complete β-PPP molecule (Figure 2), allowing the geometry of binding to be determined with confidence. As judged by comparison with the density of equivalent enzyme side chains, the occupancy of the inhibitor in the active site was estimated to be about 70%.

In Figures 1 and 2, the direction of view is approximately parallel to the c axis. In Figure 3, which illustrates the geometry of binding of β-PPP to thermolysin, inferred from the electron density maps, the view is perpendicular to c and is from the left of Figures 1 and 2.

β-PPP binds to thermolysin with the carbonyl oxygen of its peptide bond 2.1 Å from the zinc, displacing a water molecule. Although somewhat distorted, the coordination about the zinc is approximately tetrahedral. The carbonyl carbon is 3.9 Å from the side chain of Glu-143 and 3.8 Å from N^{ϵ} of His-231. Also close to the carbonyl carbon (3.5 Å) is a water molecule which forms a hydrogen bond to the imido nitrogen of Trp-115 (2.7 Å) and probably another with the carboxyl group of Glu-143 (3.1 Å). This water molecule may be of importance in catalysis, as will be discussed below. The nitrogen of the peptide bond in β-PPP participates in a hydrogen bond with the carbonyl oxygen of Ala-113, approximately 3.0 Å away.

The free carboxyl of β-PPP also participates in hydrogen bonding, one oxygen forming a salt link to Arg-203 (2.9 Å) and the other to N^{δ} of Asn-112 (2.8 Å). The side chain of Asn-112 appears to move somewhat in order to relieve a close contact between O^{δ} and C^{β} of β-PPP. Thus, all the hydrogen-bonding potential of the inhibitor appears to be satisfied.

The β-PPP phenylalanyl phenyl ring binds between the side chains of Leu-202 and Val-139, in the "hydrophobic pocket" described previously (Colman et al., 1972). This cavity is lined by the entirely nonpolar side chains and α carbons of Phe-130,

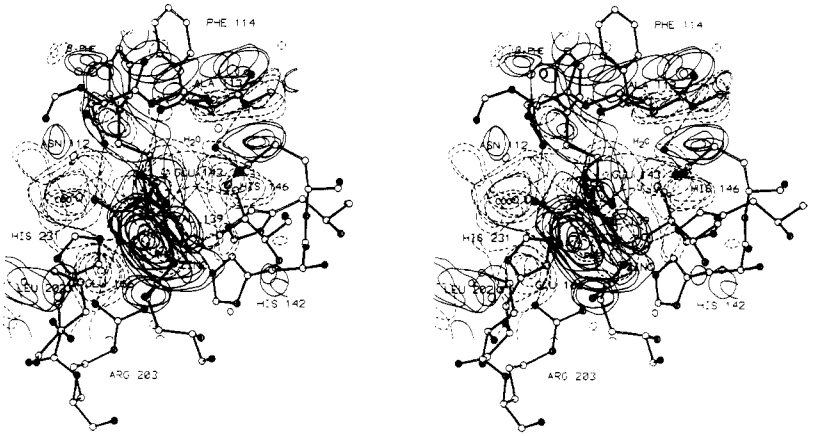

FIGURE 1: View of the active site region of the 2.3 Å resolution difference electron density map for β-PPP calculated with coefficients $F_{\beta\text{-PPP}} - F_{\text{Nat}}$. Sections $z = 1/180$ to $-12/180$. The volume shown in this map is essentially the same as in Figures 2 and 4. In this and all other maps, the contours are drawn at arbitrary equal intervals, with negative contours broken. The structures of the protein and the bound inhibitor are superimposed. Carbon atoms are indicated by open circles and oxygen by solid circles, and nitrogen atoms are hatched. The bonds of the inhibitor are drawn solid, as is the backbone of the protein. The labels for the inhibitor are smaller than those for the protein.

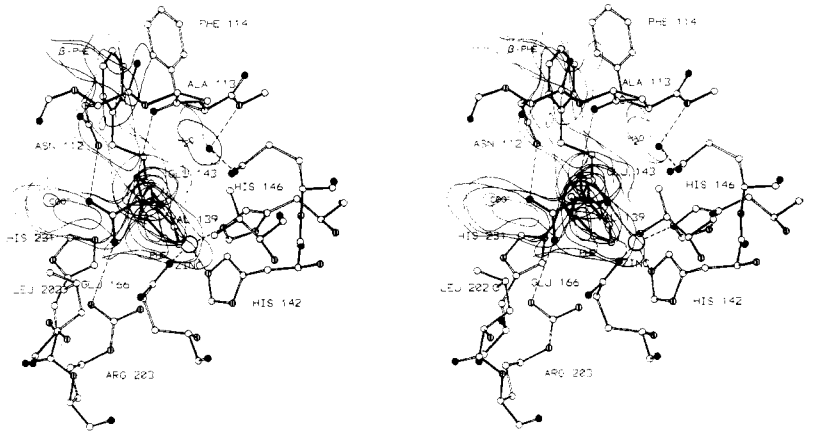

FIGURE 2: Electron density map for the β-PPP–thermolysin complex calculated with coefficients $2F_{\beta\text{-PPP}} - F_{\text{Nat}}$. For clarity, the density for the protein structure, including the zinc atom, is not shown.

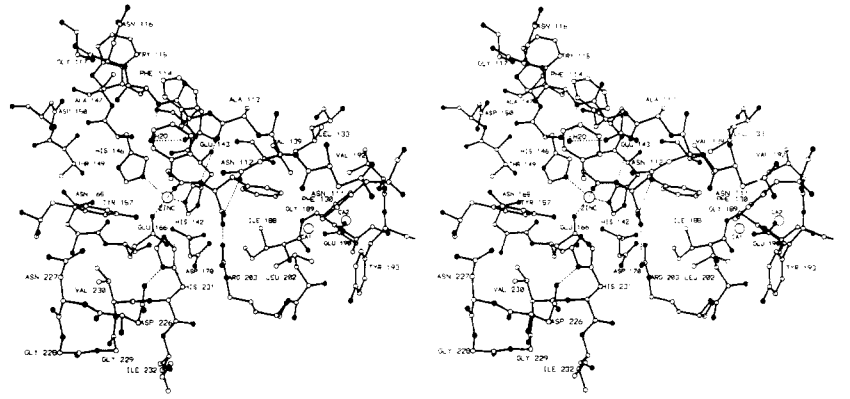

FIGURE 3: Stereoview of the inhibitor β-PPP in the thermolysin active site. The view is from the left of Figure 2. The bonds of the inhibitor are drawn solid, as is the backbone of the protein. Open circles represent carbon, solid circles oxygen, and hatched circles nitrogen atoms.

Leu-133, Val-139, Ile-188, Gly-189, Val-192, and Leu-202. From the $F_{\beta\text{-PPP}} - F_{\text{Nat}}$ difference map, it is clear that the side chain of Leu-202 rotates ~120° about its C^{β}–C^{γ} bond away from the phenyl ring. If the Leu-202 side chain were to remain in the native conformation, one of its methyl groups would be within 3 Å of the ring.

The β-propionyl phenyl ring of β-PPP lies with its plane very nearly parallel to that of Phe-114, at a distance of about 3.7 Å, participating in an apparently favorable stacking interaction.

The $F_{\beta\text{-PPP}} - F_{\text{Nat}}$ difference map (Figure 1) shows that the binding of β-PPP causes little change in the protein conformation other than localized changes in the orientations of active site residues, the largest of which, for Leu-202, has already

been described. The side chain of Glu-143 and the main chain between Phe-114 and Asn-112 also appear to move, but only slightly (<0.3 Å) in the direction of negative x (vertical in all drawings), away from the inhibitor. When the $2F_{\beta\text{-PPP}} - F_{\text{Nat}}$ map was superimposed upon the native TLN model in the Richards box, very little change could be noted in the positions of almost all side chains and the entire main chain, so that new coordinates were measured only for Leu-202 and Asn-112. The distances stated earlier refer to the native coordinates of TLN, reported previously (Matthews et al., 1974). Table III lists the final, idealized coordinates of β-PPP, together with the raw coordinates of atoms in the Leu-202 and Asn-112 side chains which differ from the native coordinates.

Binding of Cbz-Phe. The chemical structure of Cbz-Phe differs from that of β-PPP only in the substitution of an oxygen for the propionyl α carbon, yet this almost isostructural change is enough to promote a radically different mode of binding. Unlike β-PPP and the other dipeptide inhibitors, the $F_{\text{Cbz-Phe}} - F_{\text{Nat}}$ difference map has a single continuous positive density feature extending across the active site (Figure 4a). Although the density within this feature is up to three times that of the highest background peaks, the effects of solvent displacement from the active site again complicated the interpretation, so that as before a map with coefficients $2F_{\text{Cbz-Phe}} - F_{\text{Nat}}$ was used for model building. This map (Figure 4b) revealed that occupancy was essentially complete. As had been done for β-PPP, model building was attempted for two different modes of binding, one the same as for β-PPP and the second with the inhibitor "reversed." In this case, it was found that Cbz-Phe binds in the "opposite" orientation relative to β-PPP, with the two phenyl rings interchanged, and the carboxyl group bound to the zinc (Figure 5).

Although Cbz-Phe interacts with the same enzyme side chains as β-PPP, the details of these interactions are substantially different. The C-terminal carboxyl group binds with one oxygen 2.1 Å from the zinc, which again has approximately tetrahedral coordination, while the other oxygen appears to interact with Glu-143 (2.8 Å away). About 3.5 Å from the second oxygen, a water molecule binds in virtually the same position as that seen in the β-PPP–thermolysin complex.

The Cbz-Phe phenylalanyl phenyl ring occupies a position substantially different from that of the β-PPP propionyl phenyl ring. In Cbz-Phe, this group is inclined at an angle rather than stacked adjacent to the side chain of Phe-114. The amido nitrogen of Cbz-Phe is the only atom of this inhibitor which has the same role in binding as the corresponding atom in β-PPP, hydrogen-bonding to the carbonyl of Ala 113, at a distance of 2.7 Å. Again, the peptide chain near Ala-113 is perturbed somewhat toward negative x. The carbonyl group of Cbz-Phe, on the other hand, has a very different role than that of β-PPP, and interacts with Arg-203, via a water molecule. The carbobenzoxyl group of Cbz-Phe occupies the hydrophobic pocket between Val-139 and Leu-202. As in β-PPP, the side chain of Leu-202 rotates about 120° around its C^{β}–C^{γ} bond. The finding that β-PPP and Cbz-Phe bind in different modes to thermolysin has also been indicated by NMR studies of the binding of these inhibitors to the manganese-substituted enzyme (Bigbee and Dahlquist, 1974).

It is of interest to note the stereochemistry around the ester oxygen of the carbobenzoxyl group, the point at which the structure of Cbz-Phe differs from that of β-PPP. This oxygen is only 3.3 Å from the nitrogen of Ala-113 and forces the amide side chain of Asn-112 to swing out about 2 Å into the solvent. Even with this movement, the ester oxygen is still 3.0 Å from N^{δ} of Asn-112, which is probably too short to allow a group as bulky as a methylene at this position, explaining why β-PPP does not bind in the same manner as Cbz-Phe. If this argument is correct, it would imply that the side chain of Asn-112 is important not only because it interacts favorably with a productively bound substrate, but also because it prevents polypeptide substrates from binding in a nonproductive mode. The idealized coordinates for Cbz-Phe and for the Asn-112 and Leu-202 side chain atoms which move on inhibitor binding are listed in Table IV.

TABLE III: Idealized Coordinates for β-PPP.[a]

	X	Y	Z
β-Phenyl propionyl			
CA	50.8	18.4	−7.5
C	51.9	18.5	−6.5
O	52.9	19.2	−6.8
CB	50.2	17.0	−7.6
CG	48.7	17.0	−7.6
CD1	48.0	16.5	−6.5
CE1	46.6	16.5	−6.6
CZ	45.9	17.0	−7.7
CD2	48.0	17.5	−8.7
CE2	46.6	17.6	−8.7
Phenylalanine			
N	51.7	18.0	−5.3
CA	52.7	18.1	−4.2
C	53.4	16.8	−4.0
O1	52.8	15.8	−4.2
O2	54.7	16.8	−3.8
CB	52.0	18.5	−2.9
CG	52.9	18.6	−1.8
CD1	54.0	19.5	−1.7
CE1	54.8	19.7	−0.6
CZ	54.5	18.9	0.5
CD2	52.7	17.8	−0.6
CE2	53.4	18.0	0.5
H_2O	50.4	21.4	−8.0
Leu 202			
CG	56.5	14.9	0.9
CD1	56.8	14.4	−0.5
CD2	56.0	13.6	1.6
Asn 112			
CG	49.2	15.7	−3.3
ND	50.2	16.1	−3.2
OD	48.9	15.4	−4.6

[a] Coordinates are in Å relative to the orthogonal coordinate frame used previously (Matthews et al., 1974).

The idealized coordinates for Cbz-Phe and for the Asn-112 and Leu-202 side chain atoms which move on inhibitor binding are listed in Table IV.

Binding of Ala-Phe, PPN, and L-Phe. Data collection for these inhibitors was confined to subsets only and the resulting difference maps were compared directly with the β-PPP and Cbz-Phe difference maps.

The Ala-Phe map bears many resemblances to that of β-PPP. The largest positive feature, by a factor of two, occurs in the hydrophobic pocket at almost the same position as for the phenylalanyl phenyl ring of β-PPP, and obviously corresponds to the phenylalanyl side chain. There are also negative features in the Ala-Phe map similar to those in the β-PPP map attributed to solvent displacement. At the position of the propionyl side chain of β-PPP, there is a small positive feature in the Ala-Phe map which may be due to the alanine α and β carbons or could indicate a second mode of binding with low occupancy.

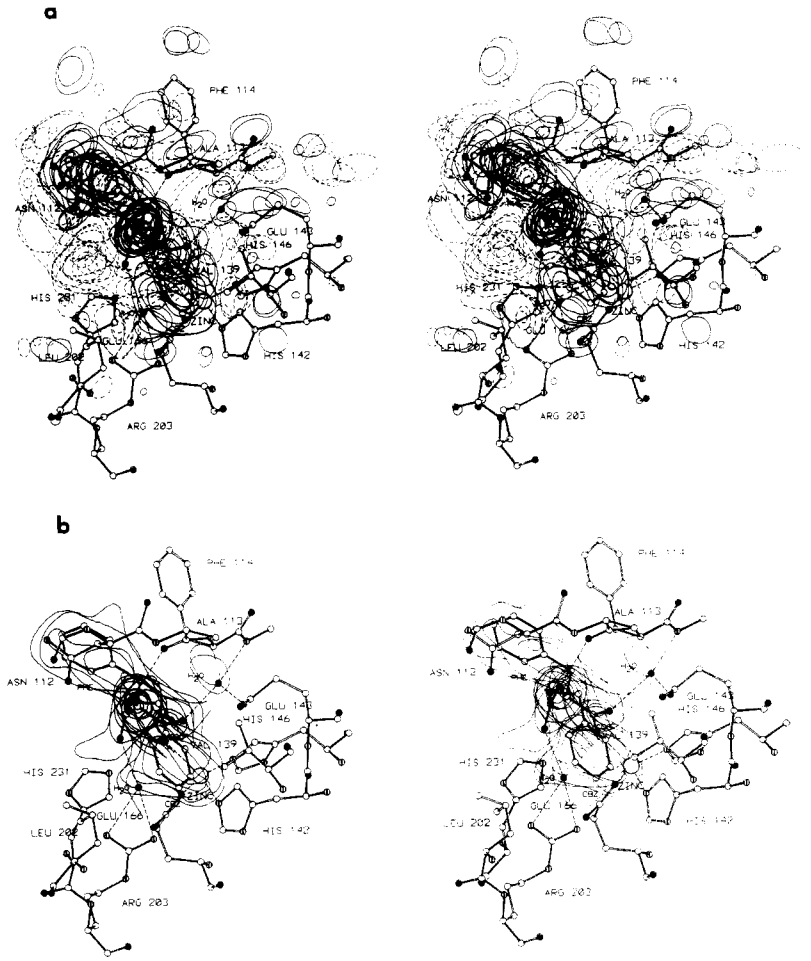

FIGURE 4: (a) Difference electron density map calculated with coefficients $F_{Cbz\text{-}Phe} - F_{Nat}$ in the vicinity of the active site. (b) Electron density map with coefficients $2F_{Cbz\text{-}Phe} - F_{Nat}$ for the Cbz-Phe–thermolysin complex. For clarity, the protein density is omitted.

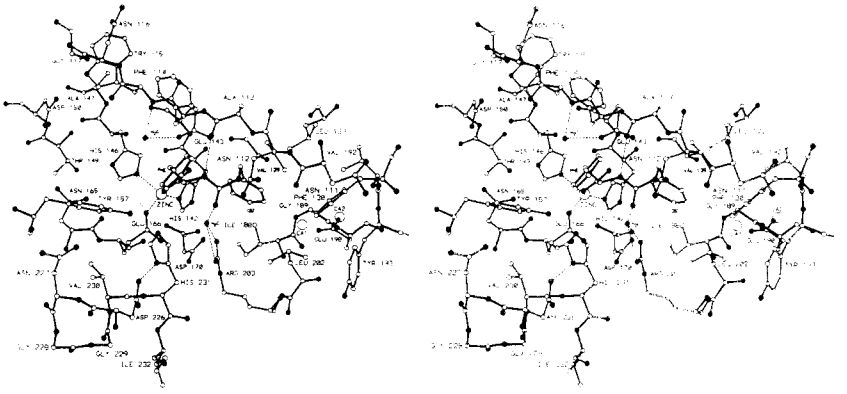

FIGURE 5: Stereodrawing showing the inferred mode of binding of Cbz-Phe within the thermolysin active site. The direction of view is from the left of Figure 4. Note that the binding is "backward" relative to that of β-PPP, shown in Figure 3.

The main conclusion, however, is that Ala-Phe binds in essentially the same manner as β-PPP.

The PPN subset difference map also resembles that of the β-PPP map more than that of Cbz-Phe. The densities for both phenyl rings correspond closely to those for β-PPP, and there is no strong negative feature at Asn-112 which would indicate that this side chain had moved as it does on binding Cbz-Phe. Therefore, PPN binds in the same mode as β-PPP and Ala-Phe. In one respect, the PPN map appears more similar to Ala-Phe than β-PPP. The position of the phenyl ring bound in the hydrophobic pocket seems to be nearly identical for PPN and Ala-Phe; however, the ring adjacent to Phe-114 appears to be tilted away somewhat in the case of PPN, possibly due to the free amino terminus of PPN. The largest differences, however, between the PPN map and the maps for β-PPP and Ala-Phe occur around the Arg-203–Asp-170 salt link and the side chain of Asn-112 and are presumably due to the substitution of the amide for the free carboxyl.

Unexpectedly, the L-Phe subset difference map is also similar to that of β-PPP even though the inhibitor has only a single aromatic group. It appears that at high concentrations (0.1 M) two molecules of L-Phe occupy the active site cleft.

TABLE IV: Idealized Coordinates for Cbz-Phe in Å.

	X	Y	Z
Carbobenzoxy			
OA	51.2	16.9	−2.6
C	51.7	16.9	−3.9
O	52.9	16.5	−4.1
CB	51.3	18.3	−2.0
CG	52.7	18.6	−1.6
CD1	53.5	19.5	−2.3
CE1	54.8	19.7	−1.9
CZ	55.3	19.1	−0.8
CD2	53.2	17.9	−0.5
CE2	54.5	18.2	−0.1
Phenylalanine			
N	50.9	17.3	−4.8
CA	51.4	17.5	−6.2
C	52.3	18.7	−6.2
O1	53.1	18.8	−7.2
O2	52.2	19.6	−5.3
CB	50.2	17.7	−7.1
CG	49.4	16.4	−7.2
CD1	48.2	16.3	−6.4
CE1	47.5	15.1	−6.4
CZ	47.9	14.1	−7.3
CD2	49.7	15.5	−8.1
CE2	49.0	14.3	−8.2
H_2O1	55.2	17.4	−4.4
H_2O2	50.4	21.4	−8.0
Leu 202			
CG	56.5	14.9	0.9
CD1	56.8	14.4	−0.5
CD2	56.0	13.6	1.6
Asn 112			
CG	49.0	14.3	−2.7
OD	48.2	13.1	−2.7
ND	50.1	14.1	−3.1

One molecule binds with its phenyl ring in the hydrophobic pocket, and, although solvent displacement obscures the density for the amino and carboxylate groups, it is likely that the carboxyl binds near Arg-203, similarly to the carboxyl of β-PPP. The second molecule binds near the zinc with its phenyl ring approximately parallel to Phe-114, in the same position as seen for the β-PPP propionyl phenyl ring. There is density indicating an interaction with the zinc (most likely the carboxyl group) and with Glu-143. Thus, although the results are somewhat ambiguous, in part due to the displacement of solvent density, it appears that two molecules of L-Phe occupy essentially the same pair of sites as are occupied by one molecule of β-PPP.

Binding of Substrates. The modes of binding observed for the various inhibitors suggest how substrates are likely to bind to TLN. Using the measured coordinates of these inhibitors as a starting point, attempts were made to fit a model of an extended substrate (Figure 6) into the TLN active site. When attempted using the Cbz-Phe coordinates, it was impossible to avoid close contacts of 2 Å or less between the extended substrate and various enzyme side chains. The steric restrictions near Asn-112 have already been pointed out in the discussion of Cbz-Phe binding. On the other hand, with the β-PPP coordinates as a starting point, the substrate model could be aligned in the active site very reasonably with only a small change in the placement of the phenyl ring near Phe-114.

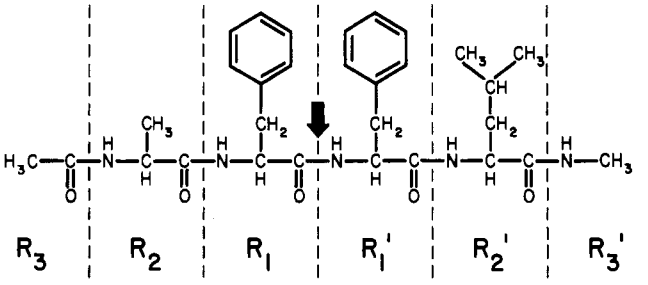

FIGURE 6: Structure of the extended substrate used for model building experiments, showing the nomenclature used to identify subsites.

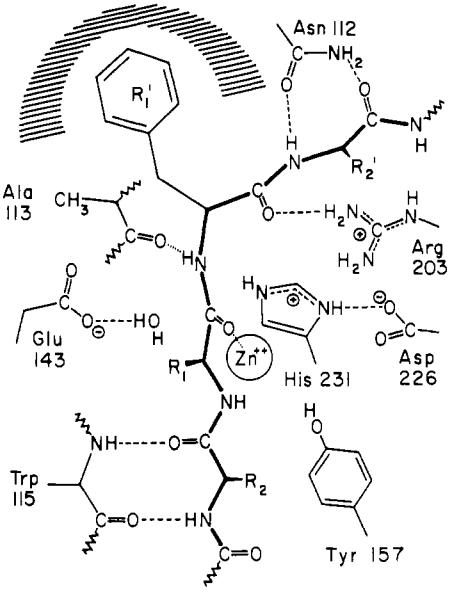

FIGURE 7: Schematic drawing illustrating the binding of an extended substrate to thermolysin, inferred from the binding of inhibitors.

In fitting the substrate model, the modes of binding for residues R_1 and R_1' were inferred from the binding of β-PPP, Ala-Phe, and PPN. The placement of residues R_2 and R_3 was determined from model-building alone, while direct evidence for the geometry of binding of residues R_1' and R_2' is provided by the analysis of phosphoramidon-inhibited TLN described elsewhere (Weaver et al., 1977).

The proposed mode of binding for extended substrates is illustrated in Figures 7 and 8. On the amino side of the scissile bond, residue R_1 and the scissile bond itself participate in essentially the same interactions as observed in the binding of β-PPP, except that the R_1 phenyl ring is tilted slightly away from Phe-114. In addition a hydrogen bond is possible between the imido nitrogen and the phenolic oxygen of Tyr-157. The backbone of residue R_2 is in a position to form two hydrogen bonds to the protein backbone of Trp-115. In fact the substrate residues R_2, R_1, and R_1' interact with the protein backbone between Trp-115 and Ala-113 as in an antiparallel pleated sheet. Although model building was carried out with an alanine as residue R_2, larger side chains could be accommodated at this site. Model building was not attempted beyond the α carbon of residue R_3 as there are no obvious favorable interactions which might occur beyond this point.

The water molecule associated with Glu-143 in the β-PPP–TLN structure cannot occupy the same position if the backbone carbonyl of R_2 hydrogen-bonds to the imide nitrogen of Trp-115. Therefore, the water molecule either must move

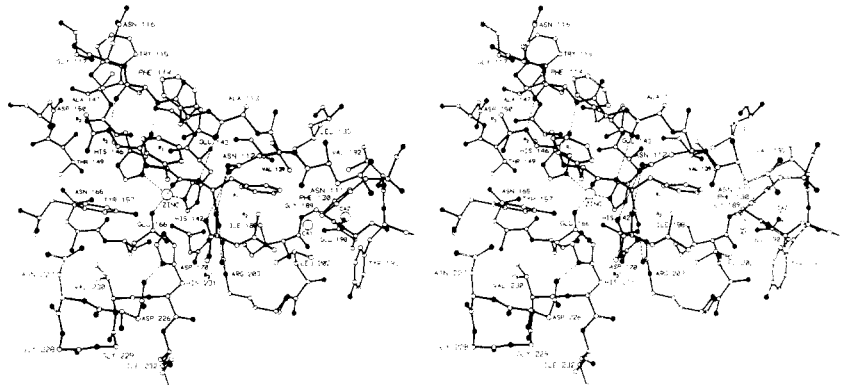

FIGURE 8: Stereodrawing showing the presumed orientation of an extended substrate in the active site of thermolysin.

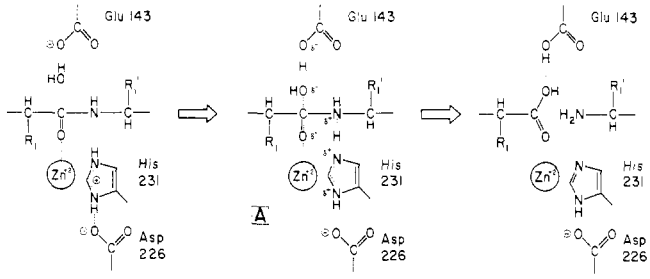

FIGURE 9: Schematic illustration of the proposed mechanism of action of thermolysin.

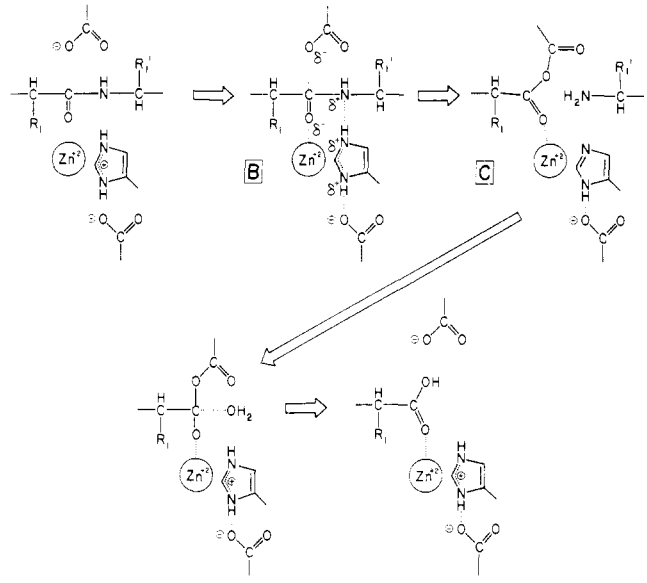

FIGURE 10: An alternative mechanism for thermolysin.

to a position between Glu-143 and the Zn-bound carbonyl of the substrate (such a movement could be accommodated by a small rotation around the Glu-143 C^{α}–C^{β} bond) or be displaced entirely. These two possibilities are important in considering the mechanism of action and are discussed below.

On the carboxyl side of the scissile bond, the peptide bond joining R_1' and R_2' binds between Arg-203 and Asn-112, very similarly to the free carboxyl of β-PPP. The carbonyl oxygen hydrogen-bonds to Arg-203, while the nitrogen is in an excellent position to hydrogen-bond to the amide oxygen of the side chain of Asn-112.

As inferred from the binding of phosphoramidon (Weaver et al., 1977), the side chain of Asn-112 rotates slightly about its C^{α}–C^{β} and C^{β}–C^{γ} bonds to make this hydrogen bond more reasonable and also to form another hydrogen bond between the amide nitrogen and the carbonyl of R_2'. The R_2' side chain then binds next to a small hydrophobic "patch" formed by Leu-202, Phe-130, and Tyr-193. This area will easily accommodate large side chains, such as tryptophan, as is the case for phosphoramidon. Model building does not suggest any obvious interactions involving residue R_3'.

Discussion

Mechanism of Action. The stereochemistry of the binding of the thermolysin inhibitors described above suggests a mechanism of action for the enzyme which is illustrated schematically in Figure 9. As will be apparent, the mechanism proposed here is similar in a number of respects to that proposed by Lipscomb and co-workers for carboxypeptidase A (Lipscomb et al., 1968, 1969, 1970) and also includes features of the thermolysin mechanism suggested by Pangburn and Walsh (1975).

The mechanism which we favor and other mechanisms which may be considered are all based upon the action of three groups on the enzyme: Glu-143, His-231, and the zinc. The zinc is essential for activity (Latt et al., 1969) and the other two groups are the closest side chains to the scissile peptide bond which may reasonably be expected to participate in hydrolysis. The proposed mechanism may be summarized as follows:

(1) Following substrate binding, Glu-143 promotes the nucleophilic attack of a water molecule upon the carbonyl carbon of the scissile peptide bond, which has already been somewhat depolarized by the zinc.

(2) Concurrent with or following step 1, His-231 donates a proton to the peptide nitrogen, forming an intermediate which is tetrahedral at both the carbon and nitrogen of the scissile bond. This intermediate is stabilized by the hydrogen bonds with Glu-143 and His-231 which still remain.

(3) The carbon–nitrogen bond of the intermediate then breaks to yield the products.

An alternative mechanism is shown in Figure 10. In this case, Glu-143 attacks the carbonyl carbon directly, rather than through a water molecule. A tetrahedral intermediate is formed, which, following donation of a proton from His-231, releases the leaving group to form an anhydride intermediate. The anhydride is subsequently hydrolyzed by a water molecule to yield the final products. In the alternate mechanism, the roles of His-231 and the zinc are very similar, but the role of Glu-143 is different.

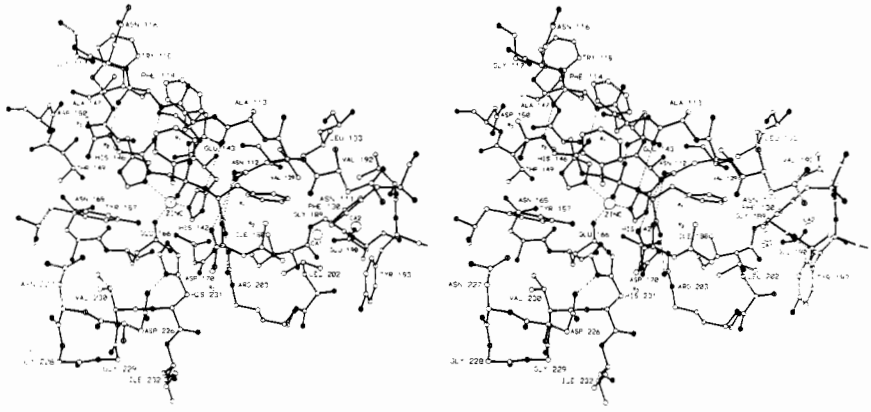

FIGURE 11: Stereodiagram showing the binding of the presumed tetrahedral transition state intermediate to thermolysin.

The alternative schemes outlined above are clearly similar to those postulated for carboxypeptidase A (Lipscomb et al., 1968, 1969, 1970). Glu-143 of TLN appears to be a counterpart of Glu-270 in carboxypeptidase A, as anticipated previously (Colman et al., 1972), while the role of His-231 in TLN as a proton donor is analogous to the role of Tyr-248 in carboxypeptidase A, as also suggested by Pangburn and Walsh (1975). A detailed comparison of the active sites of TLN and carboxypeptidase A will be presented elsewhere, but for the moment it may be noted that the binding of dipeptides to TLN is very similar to that of, for example, glycyltyrosine to carboxypeptidase A, although no major movements are observed in any thermolysin side chains, as is the case with Tyr-248 and Arg-145 of carboxypeptidase A.

Although it has not been possible to date to differentiate between the mechanisms of Figures 9 and 10 above as favored mechanisms for the metalloproteases, the following structural considerations suggest that the mechanism of Figure 9 is more plausible for thermolysin. As mentioned earlier, when β-PPP is bound to TLN, the closest oxygen of Glu-143 is 3.9 Å from the carbonyl carbon of the scissile bond. Inspection of the complex (Figure 8) shows that Glu-143 cannot be brought closer by rotations about side-chain bonds. Also the backbone of Glu-143, being in an internal helix, is not free to move. On attempting to build models of intermediates which would be formed in the case of the mechanism of Figure 9, it was found that the tetrahedral intermediate (A) could be made to fit very reasonably in the active site with a minimum of change from the positions proposed for substrate binding (Figure 11). Each of the hydrogen bonds can be preserved, and there appear to be no prohibitive van der Waals contacts. Also, the proposed hydrogen bond with Glu-143 has a length of 2.5–2.7 Å and the appropriate stereochemistry. The change from planar to tetrahedral geometry at the carbonyl carbon causes the side chain of R_1 to move closer to Phe-114, into approximately the same position as the equivalent group in the β-PPP structure, "stacking" next to the Phe-114 side chain. Also, when the nitrogen of the scissile peptide becomes tetrahedral, it moves ~0.7 Å closer to His-231. In summary there is no stereochemical reason to exclude the mechanism in Figure 9.

On the other hand, model building suggests that the mechanism in Figure 10 is implausible. In order to form intermediate (B), the tetrahedral carbon of the hydrolyzed bond has to be brought 1–1.5 Å closer to Glu-143, resulting in a number of close contacts. The R_1 phenyl group would have to undergo a major reorientation in order to prevent contacts of 2–3 Å with the Phe-114 side chain, and also the hydrogen bond between the R_2 carbonyl and the Trp-115 nitrogen would be shortened to about 2 Å. Also, coordination around the zinc would become very distorted, and the nitrogen of the scissile bond would move farther away from His-231, to a separation of about 5 Å. Similarly, model building of the anhydride intermediate (C) indicates that it would be in a very high-energy conformation. The zinc–oxygen ligand distance would be stretched to about 2.8 Å at the minimum, and the R_1 α carbon would be only 2 Å from C^β of Phe-114. Since all of the close contacts seen for intermediates B and C are with relatively immobile main chain and C^β atoms, a major change in the conformation of the active site would have to be postulated for the mechanism in Figure 10 to be possible. For this reason we favor the mechanism in Figure 9.

The binding of dipeptide inhibitors and the model-building studies based on them suggest that a number of groups participate in substrate binding and may also contribute significantly toward stabilization of the transition state. Figures 7, 8, and 11 illustrate the presumed hydrogen-bonded interactions of the substrate upon initial binding and in the transition state. All of the available hydrogen-bond donors and acceptors of the substrate appear to interact with the enzyme. Three of these bonds are with main-chain atoms of the enzyme and four with side chains.

Hydrophobic interactions also are important in forming the Michaelis complex and possibly in stabilizing the transition state. The largest contribution seems to come from the binding of the R_1' side chain in the hydrophobic pocket. At this site, the interactions appear to be substantially the same for the initial substrate binding mode and for the transition state. On the other hand, the hydrophobic interaction between the R_1 side chain and Phe-114 may increase in the transition state. The β-PPP–thermolysin complex indicates that the most favorable orientation of R_1 is "stacked" next to Phe-114. When attempts were made to model-build an extended substrate, it was found that the additional stereochemical restrictions imposed by adding residue R_2 necessitated a shift of the R_1 side chain away from Phe-114. This shift was also indicated in the subset difference map for the Phe-Phe-amide where, in contrast to β-PPP, R_1 has the amino group present. When the transition state model was fit into the active site, the altered geometry of the peptide bond was seen to allow R_1 to occupy the stacked positon next to Phe-114. This interaction might lower the free-energy barrier of the transition state for substrates in which R_1 is hydrophobic and bulky.

Upon the binding of substrates (Figure 8), Glu-143 becomes completely buried in a nonpolar environment, and we assume that a water molecule must also be buried along with it. At neutral pH, Glu-143 is expected to be charged, and the high

free-energy required to bury this group must be provided by the favorable interactions described above. Under these conditions, Glu-143 becomes a strong base capable of mediating the attack of the water molecule upon the carbonyl carbon of the susceptible peptide bond. Formation of the tetrahedral transition state would be promoted by a lowering of the free energy of Glu-143 on neutralization and the transfer of the charge to the zinc-bound oxygen. Thus, the initial "burial" of Glu-143 may be one of the driving forces of catalysis, as has also been postulated for carboxypeptidase (Lipscomb et al., 1969).

The stereochemistry of β-PPP binding indicates that His-231 is in a favorable position to act as a proton donor, N^{ϵ} of the imidazole being about 4.2 Å from the nitrogen of the scissile bond. Also, in both the native structure and the inhibited complexes, N^{δ} of this histidine hydrogen-bonds to the carboxyl of Asp-226 to form a complex reminiscent of the "charge relay system" observed in the serine proteases (Blow et al., 1969). One might therefore expect the pK of this group to be somewhat higher than that of a "normal" histidine, so that it should be protonated at neutral pH. However, one cannot press too closely the analogy of the "charge relay system", as in thermolysin both the imidazole and aspartate are largely exposed to solvent. The distance of 4.2 Å from His-231 to the peptide nitrogen indicates that a hydrogen bond does *not* exist between these groups. This is as expected, since an amide nitrogen cannot act as an acceptor of a hydrogen bond (Sundberg and Martin, 1974). Model building of the transition state intermediate suggests that as the carbonyl carbon and the nitrogen of the scissile bond both become tetrahedral, the nitrogen moves to within about 3.5 Å of $N^{\epsilon 2}$ of His-231. The geometry is such that a small movement of His-231 can then bring $N^{\epsilon 2}$ 0.5 Å closer to the substrate with the $N^{\epsilon 2}$–proton bond pointed directly at the "lone pair" of the newly tetrahedral nitrogen. Therefore, on stereochemical grounds, direct proton transfer seems likely, although one cannot exclude the possibility of proton transfer via a water molecule.

The role of the zinc in thermolysin appears to be very similar to that of the metal in carboxypeptidase A. The carbonyl oxygen of the scissile peptide bond binds directly to the zinc at a distance of ~2.1 Å to make the zinc coordination approximately tetrahedral. As suggested earlier by Lipscomb and co-workers in discussions of the carboxypeptidase A mechanism, the role of the zinc could be not only to align the peptide in the optimal orientation, but also to aid in polarizing the carbonyl bond (Lipscomb et al., 1968, 1969, 1970; Quiocho and Lipscomb, 1971). The binding of the carbonyl may be seen as a "burial" of the charged zinc ion in a relatively nonpolar medium, as compared with the binding of a water molecule and associated solvent in the absence of substrate. The zinc could then act as a Lewis acid and in concert with Glu-143 cause the formation of the tetrahedral carbon. The zinc may also be particularly important in stabilizing the transition state by an electrostatic interaction with the negatively charged oxygen.

In Figure 9 the mechanism is illustrated as one in which Glu-143, His-231, and the zinc act in a concerted fashion. Alternatively, one may conceive of the mechanism as a stepwise one in which, first, the zinc polarizes the carbonyl, second, the carbonyl carbon becomes tetrahedral by the addition of the water molecule, and finally, His-231 donates a proton to the nitrogen. The present experiments do not resolve this ambiguity.

pH Dependence of Activity. The mechanism for thermolysin proposed above is based primarily on the crystallographic observations but is also consistent with a variety of chemical data which will be summarized in this and the following sections.

The optimum activity for thermolysin and the related neutral proteases has been shown by a number of investigators to occur near pH 7.0 (e.g., see Tsuru et al., 1966; Feder and Schuck, 1970; Pangburn and Walsh, 1975). Pangburn and Walsh (1975) have shown that thermolysin activity depends on two groups, an unprotonated species with a pK_a of 5.9 which they propose to be Glu-143, and a protonated species with a pK_a of 7.5 which they propose to be His-231. The identification of His-231 as a proton donor rests primarily on studies of the inhibition of thermolysin with ethoxyformic anhydride (Blumberg et al., 1973, 1974; Burstein et al., 1974). Although direct proof is lacking, a variety of evidence indicates that this inhibitor acylates His-231 (crystallographic experiments indicated that ethoxyformic anhydride reacts with His-216, 25 Å from the active site, but did not reveal the site responsible for inhibition, partly due to the fact that a maximum of 25% inhibition could be obtained with large crystals suitable for x-ray analysis (S. J. Remington and B. W. Matthews, unpublished results)). The identification of Glu-143 as the unprotonated species with pK_a of 5.9 rests exclusively on its location in the thermolysin active site.

On the basis of the above considerations Pangburn and Walsh have already proposed the general base mechanism, which we favor, or direct nucleophilic attack by Glu-143, as alternative mechanisms for the action of thermolysin.

Inhibitions by Metal Ions. A number of metal ions, including Hg^{2+}, Zn^{2+}, and Ag^{+}, have been shown to inhibit thermolysin (Endo, 1962; Holmquist and Vallee, 1974; Pangburn and Walsh, 1975).

The binding sites for Zn^{2+} and Ag^{2+} were determined crystallographically by calculating difference Fourier projections (Figure 12) for crystals soaked respectively in 0.01 M $ZnCl_2$, pH 7.0, and 0.005 M $AgNO_3$, pH 6.0, in standard mother liquor. In addition, the sites of binding of free mercury and of dimercury acetic acid (DMA) had been determined during the thermolysin structure refinement.

Each of the metals is complexed by His-231, and in the case of Zn^{2+} and Hg^{2+}, apparently also by the phenolic oxygen of Tyr-157. As mentioned previously (Colman et al., 1972), Ag^{+} also binds with variable occupancy at His-88. Zn^{2+} appears to occupy two alternative positions, one similar to that for Hg^{2+}, and the second such that the metal is complexed by His-231 and Asn-112. For DMA, Hg^{2+}, Zn^{2+}, and Ag^{+}, the position occupied by the metal is in each case within no more than 3 Å from the presumed position of the R_1 α-carbon atom of a substrate, almost certainly resulting in competitive binding of inhibitor and substrate. Thus, inhibition on the binding of these metals to His-231 is consistent with this group participating in catalysis, but does not constitute proof.

Inhibition by Dipeptides. A number of studies have shown that thermolysin is inhibited by substrates containing either a free amino terminus at R_1 or a free carboxyl terminus at R_1' (Matsubara, 1966; Morihara, 1967; Morihara and Tsuzuki, 1970; Feder et al., 1974, 1976). While substrates with a free carboxyl group may be hydrolyzed slowly, no cleavage at all is observed in the presence of a free amino terminus.

The difference maps calculated with partial data sets for Ala-Phe and Phe-Phe-amide indicate that these dipeptides bind similarly to β-PPP, i.e., as an extended substrate (cf. Figure 3). Assuming this to be the case, the free amino group of residue R_1 would be in an ideal position to hydrogen-bond to the water molecule bound to Glu-143, or might interact directly

with this acid group. In either event, hydrolysis of the substrate would not occur since Glu-143 and its associated water molecule would not be "buried" as for an extended substrate. A similar interference with Glu-270 in carboxypeptidase A is thought to cause glycyl-L-tyrosine to be very poor substrate for this enzyme (Hartsuck and Lipscomb, 1971). For thermolysin substrates, blocking of the N terminus with an acetyl group does result in hydrolysis (Morihara et al., 1968), suggesting that this group is sufficient to provide the correct environment for Glu-143, and also that the formation of the hydrogen bond from the R_2 carbonyl oxygen to the protein backbone at Trp-115 may be essential for catalysis.

Reduction in the rate of catalysis by a free carboxyl group could be due to a number of causes. For example, the carboxyl group would be close enough to His-231 that there could be an electrostatic interaction between them hindering the action of this group. The presumed interaction between His-231 and the free carboxyl could either be direct, or perhaps, via solvent, as we do see apparent solvent density adjacent to the carboxyl group of β-PPP (Figure 2). Also, the geometry of interaction of the free carboxyl with Arg-203 and Asn-112 is presumably slightly different than for an extended substrate, possibly contributing to nonproductive alignment.

Specificity. The specificity of thermolysin toward both protein and synthetic substrates has been analyzed by a number of investigators (e.g., see Matsubara et al., 1966; Matsubara, 1966; Morihara et al., 1968; Feder and Schuck, 1970).

Morihara and Tsuzuki (1970) carried out a detailed kinetic analysis of a series of synthetic substrates and concluded that at least three residues on the N-terminal side and two residues on the C-terminal side of the scissile bond affect catalysis. This is consistent with the extended substrate binding site shown in Figure 8. TLN is most specific for residue R_1', Leu, Ile, and Phe being most efficiently catalyzed at this position. A substrate containing Tyr at R_1' has about the same K_m as Phe, but k_{cat} is greatly reduced, and, as a result, Tyr is catalyzed at a rate only slightly faster than Ala. Catalysis with Trp at R_1' is negligible.

This apparent size restriction at the site of R_1' binding is consistent with the manner in which Phe binds in the hydrophobic pocket (Figures 3 and 8). The ring fits snugly into this depression with its C^ζ only 3.8 Å from C^α of Gly-189. Substitution of Tyr for this side chain would place the phenolic oxygen within 2.6 Å of Gly-189. Since a rotation about the C^α–C^β bond would also create further bad contacts, it appears that such a substrate must bind 0.5–1.0 Å further away from the pocket, and that this translation probably changes the substrate's interaction with the zinc and also moves the nitrogen of the scissile bond away from His-231. Substitution of Trp at R_1' would result in an even larger shift, if such a substrate could bind at all. Also, inspection of the model indicates that a substrate with a D-amino acid at R_1' must bind in a completely different orientation, if at all, consistent with the observation that such substrates are not hydrolyzed (Morihara and Ebata, 1966; Morihara, 1967; Morihara et al., 1968; Morihara and Tsuzuki, 1970).

In contrast to the limitation on R_1', the kinetic analysis of Morihara et al. (1968) suggests that there is no such size restriction for R_1. Substrates with Phe, Tyr, or Trp at R_1 are catalyzed most efficiently, and, from the results of Morihara and co-workers and the binding studies of dipeptide inhibitors by Feder et al. (1976), it is evident that Phe (the only aromatic side chain tested) binds most strongly of all side chains at this position. This is consistent with the observation that, in the

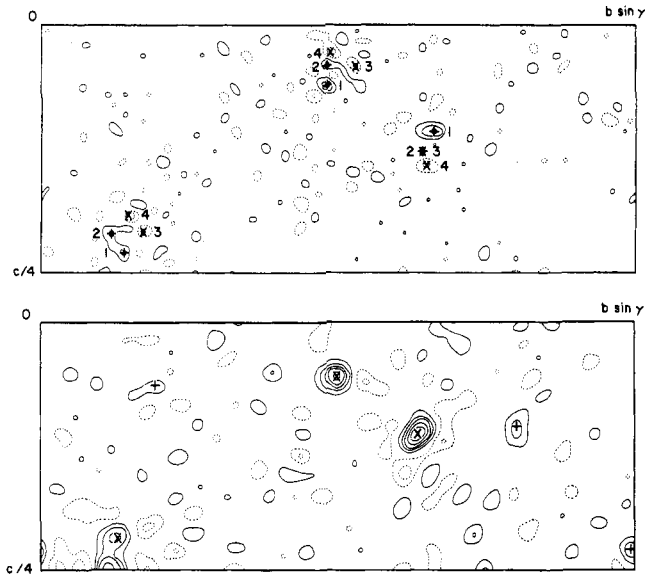

FIGURE 12: Difference Fourier projections showing the binding of zinc and silver ions to thermolysin. Each binding site appears three times within a given projection. (a, top) Zinc thermolysin minus native thermolysin map at 2.3 Å resolution. The refined coordinates for the two alternate zinc binding sites (+) are labeled 1 and 2, and two negative features due to loss of solvent (X) are labeled 3 and 4. (b, bottom) Silver thermolysin minus native thermolysin at 4.0 Å resolution. The refined position for the principal silver binding site at His-231 is marked X, and the secondary site at His-88 is marked +.

binding of β-PPP, the planar aromatic side chain "stacks" next to Phe-114, giving added stability to this complex. Again, the substitution of a D-amino acid such as D-alanine at this position completely abolishes activity (Morihara et al., 1968; Morihara and Tsuzuki, 1970). In this case the D residue could not be bound in a productive mode because of close approaches to C^β of Phe-114.

Morihara and Tsuzuki (1970) have also shown that changes in R_2 result in more complex kinetic effects. Values of K_m for a set of synthetic substrates containing Gly, Ala, and Phe at this position were 12.2, 8.6, and 0.91 mM, respectively. However, k_{cat} for the same substrates was 362.0, 5208.0, and 446.4 s^{-1}, suggesting that Phe binds the most tightly, but Ala binds in a manner most efficient for catalysis. Model building with Ala at position R_2 indicates that this side chain binds close to the imidazole of His-146 (Figure 8). It appears that the more bulky phenylalanyl side chain could be accommodated in a shallow depression near Asp-150, Asn-165, and Tyr-157, although it would not be surprising if the presence of this larger group resulted in a slight change in the overall geometry of the substrate. In this case, it appears that, with minor alterations in the alignment of the substrate, D-alanine could be bound at this site, consistent with the observation that Cbz-D-Ala-Gly-Leu-Ala is hydrolyzed (Morihara and Tsuzuki, 1970).

At R_2', there appears to be a definite preference for a hydrophobic residue. The K_m's of substrates with Leu or Phe at this position are about four times smaller than those of Ala or Gly. As before, however, Ala at R_2' gives the highest value for k_{cat}. The presumed binding of substrates with Leu at R_2', which have the largest value for k_{cat}/K_m, is shown in Figure 8 and was inferred in part from the observed binding of phosphoramidon (R_2' = Trp) (Weaver et al., 1977). As seen in the figure, there are several hydrophobic residues including Leu-202, Phe-130, and Tyr-193 which can contribute to the binding of bulky hydrophobic side chains.

Morihara and Tsuzuki (1970) also present kinetic data for

sites R_3 and R_3'. The largest effects of amino acid substitutions were on k_{cat}, with very little effect on the values of K_m. We can offer little comment on these results except to say that the binding sites for R_3 and R_3' are not well defined. As can be seen in Figure 8, a bulky side chain at R_3 would be expected to interact with the protein, whereas little if any interaction would be expected for a side chain at R_3'.

Recently Vallee and co-workers have shown that thermolysin acylated with amino acid *N*-hydroxysuccinimide esters becomes "superactive" toward certain substrates (Blumberg et al., 1973, 1974; Blumberg and Vallee, 1975). The degree of superactivation depends both on the nature of the acyl group incorporated and on the structure of the substrate. For relatively poor thermolysin substrates, acylation of the enzyme with bulky aromatic derivatives can result in a 400-fold enhancement in activity, whereas for the best substrates tested little if any enhancement was observed. Blumberg and Vallee (1975) show that the site of acylation is probably a tyrosine residue, and the most likely candidate appears to be Tyr-157. The role played by this residue in thermolysin catalysis is not yet clear. In the electron density map for the native enzyme, the density for the side chain of Tyr-157 is somewhat weak, suggesting that some rotation about the C^{α}–C^{β} bond occurs in the crystal.

The phenolic oxygen is in a position to interact either with the zinc, with Glu-166, or possibly to form a hydrogen bond to N^{ϵ} of His-231, although the bond geometry is far from ideal. When a substrate is bound, a movement of about 0.5 Å would bring the phenolic oxygen within hydrogen-bonding distance of the imino nitrogen of residue R_1, as shown in Figure 8. Because of its freedom to rotate away from the active site cleft, Tyr-157 could still be acylated in the presence of the competitive inhibitors β-PPP or Zn^{2+}, as found by Vallee and coworkers. Also, it would be reasonable to speculate that modification of Tyr-157 would alter the "specificity" of thermolysin with respect to residues R_1' and R_2', resulting in "superactive" cleavage of selected substrates; however, a definitive explanation of thermolysin superactivation must await further experimental evidence.

Acknowledgments

We are grateful to Dr. B. L. Vallee for a gift of β-phenylpropionyl-L-phenylalanine and thank Dr. Lynn F. Ten Eyck for help with a number of computational problems and Drs. F. W. Dahlquist and R. S. Roche for several helpful discussions.

References

Bigbee, W. L., and Dahlquist, F. W. (1974), *Biochemistry 13,* 3542.

Blow, D. M., Birktoft, J. J., and Hartley, B. S. (1969), *Nature (London) 221,* 337.

Blumberg, S., Holmquist, B., and Vallee, B. L. (1973), *Biochem. Biophys. Res. Commun. 51,* 987.

Blumberg, S., Holmquist, B., and Vallee, B. L. (1974), *Isr. J. Chem. 12,* 643.

Burstein, Y., Walsh, K. A., and Neurath, H. (1974), *Biochemistry 13,* 205.

Colman, P. M., Jansonius, J. N., and Matthews, B. W. (1972), *J. Mol. Biol. 70,* 701.

Endo, S. (1962), *J. Ferment. Tech. 40,* 346.

Feder, J., Auferheide, N., and Wildi, B. S. (1976), in Enzymes and Proteins from Thermophilic Microorganisms, Zuber, H., Ed., Basel, Switzerland, Birkhäuser Verlag, p 31.

Feder, J., Brougham, L. R., and Wildi, B. S. (1974), *Biochemistry 13,* 1186.

Feder, J., Garrett, L. R., and Wildi, B. S. (1971), *Biochemistry 10,* 4552.

Feder, J., and Schuck, J. M. (1970), *Biochemistry 9,* 2784.

Hartsuck, J. A., and Lipscomb, W. N. (1971), *Enzymes, 3rd Ed. 3,* 1.

Holmquist, B., and Vallee, B. L. (1974), *J. Biol. Chem. 249,* 4601.

Latt, S. A., Holmquist, B., and Vallee, B. L. (1969), *Biochem. Biophys. Res. Commun. 37,* 333.

Lipscomb, W. N., Hartsuck, J. A., Quiocho, F. A., and Reeke, G. N., Jr. (1969), *Proc. Natl. Acad. Sci. U.S.A. 64,* 28.

Lipscomb, W. N., Hartsuck, J. A., Reeke, G. N., Jr., Quiocho, F. A., Bethge, P. H., Ludwig, M. L., Steitz, T. A., Muirhead, H., and Coppola, J. C. (1968), *Brookhaven Symp. Biol. 21,* 24.

Lipscomb, W. N., Reeke, G. N., Jr., Hartsuck, J. A., Quiocho, F. A., and Bethge, P. H. (1970), *Phil. Trans. R. Soc. London, Ser. B 257,* 177.

Matsubara, H. (1966), *Biochem. Biophys. Res. Commun. 24,* 427.

Matsubara, H., Sasaki, R., Singer, A., and Jukes, T. H. (1966), *Arch. Biochem. Biophys. 115,* 324.

Matthews, B. W., Colman, P. M., Jansonius, J. N., Titani, K., Walsh, K. A., and Neurath, H. (1972a), *Nature (London), New Biol. 238,* 41.

Matthews, B. W., Jansonius, J. N., Colman, P. M., Schoenborn, B. P., and Dupourque, D. (1972b), *Nature (London), New Biol. 238,* 37.

Matthews, B. W., Klopfenstein, C. K., and Colman, P. M. (1972c), *J. Sci. Instrum. 5,* 353.

Matthews, B. W., Weaver, L. H., and Kester, W. R. (1974), *J. Biol. Chem. 249,* 8030.

Morihara, K. (1967), *Biochem. Biophys. Res. Commun. 26,* 656.

Morihara, K., and Ebata, M. (1966), *J. Biochem. (Tokyo) 61,* 149.

Morihara, K., and Tsuzuki, H. (1970), *Eur. J. Biochem. 15,* 374.

Morihara, K., Tsuzuki, H., and Oka, T. (1968), *Arch. Biochem. Biophys. 123,* 572.

Pangburn, M. K., and Walsh, K. A. (1975), *Biochemistry 14,* 4050.

Quiocho, F. A., and Lipscomb, W. N. (1971), *Adv. Protein Chem. 25,* 1.

Richards, F. M. (1968), *J. Mol. Biol. 37,* 225.

Sober, H. A., Ed., (1970), Handbook of Biochemistry: Selected Data for Molecular Biology, Cleveland, Ohio, Chemical Rubber Publishing Co., pp J4–5.

Sundberg, R. J., and Martin, R. B. (1974), *Chem. Rev. 74,* 471.

Ten Eyck, L. F., Weaver, L. H., and Matthews, B. W. (1976), *Acta Crystallogr., Sect. A, 32,* 349.

Titani, K., Hermodson, M. A., Ericsson, L. H., Walsh, K. A., and Neurath, H. (1972), *Nature (London), New Biol. 238,* 35.

Tsuru, D., Yamamoto, T., and Fukumoto, J. (1966), *Agric. Biol. Chem. 30,* 651.

Weaver, L. H., Kester, W. R., and Matthews, B. W. (1977), *J. Mol. Biol.* (in press).